Physics Faculty Research & Creative Works

Physics

01 Jan 2005

Static Pairwise Annihilation in Complex Networks

M. F. Laguna

M. Aldana

H. Larralde

V. M. Kenkre

et. al. For a complete list of authors, see *https://scholarsmine.mst.edu/phys_facwork/314*

Recommended Citation

Static pairwise annihilation in complex networks

M. F. Laguna,[1,2] M. Aldana,[1,3,*] H. Larralde,[3] P. E. Parris,[1,4] and V. M. Kenkre[1]

[1]*Consortium of the Americas for Interdisciplinary Science, University of New Mexico, Albuquerque, New Mexico USA*
[2]*Centro Atómico Bariloche, CONICET and Instituto Balseiro, San Carlos de Bariloche, Argentina*
[3]*Centro de Ciencias Físicas-UNAM, Cuernavaca, México*
[4]*University of Missouri-Rolla, Rolla, Missouri, USA*

We study static annihilation on complex networks, in which pairs of connected particles annihilate at a constant rate during time. Through a mean-field formalism, we compute the temporal evolution of the distribution of surviving sites with an arbitrary number of connections. This general formalism, which is exact for disordered networks, is applied to Kronecker, Erdös-Rényi (i.e., Poisson), and scale-free networks. We compare our theoretical results with extensive numerical simulations obtaining excellent agreement. Although the mean-field approach applies in an exact way neither to ordered lattices nor to small-world networks, it qualitatively describes the annihilation dynamics in such structures. Our results indicate that the higher the connectivity of a given network element, the faster it annihilates. This fact has dramatic consequences in scale-free networks, for which, once the "hubs" have been annihilated, the network disintegrates and only isolated sites are left.

PACS number(s): 89.75.Hc, 02.50.Ey, 05.45.−a

I. INTRODUCTION

The reaction dynamics of particles that undergo pairwise mutual annihilation is of interest to various fields of physics, including diffusion controlled reactions [1,2], and exciton annihilation in molecular crystals [3]. In these examples the particles are free to move or diffuse throughout the system, and when two complementary particles collide, they annihilate. This kind of dynamics can be modeled by adopting a network approach in which the particles, rather than moving across the system, are placed at the vertices of a given network. The edges of the network would represent direct interactions between the particles at a given time, or interactions that might occur during time as the particles diffuse throughout the system. This approach has proven to be useful in understanding the collective dynamical behavior in many-particle systems [4,5]. In some other cases, the annihilating particles can be accurately represented as being fixed on a lattice. As an example, consider the pycnonuclear reactions taking place in the interior of dense stars [6–8]. In this case, the atom nuclei undergoing mutual annihilation become frozen into a regular crystalline lattice structure due to the high densities of the cores. Other examples are the irreversible sequential adsorption and "car parking" analogs, where the system reaches a jammed state in which the lattice or space cannot be filled completely [9].

In the present paper we investigate the static pairwise annihilation problem on complex networks, generalizing previous results obtained for ordered lattices [10,11]. As such, the annihilation problem on complex networks is interesting in its own right since it provides a dynamical probe of the topological properties of the structure on which it occurs. These properties will be different than, and complementary

to, those associated with other physical processes in complex networks, such as random walks [12], Ising spin dynamics [13], target annihilation [14,15], majority voter models and neural network dynamics [16,17], epidemic spreading [18,19], trapping [20,21], etc.

It is precisely these complementary features which lead us to consider static annihilation as a probe of different complex networks, such as ordered lattices, Erdös-Rényi random networks (also called Poisson networks), scale-free networks, and small-world networks. Small-world networks are particularly interesting, since they can be considered as a class of networks lying at some intermediate point between ordered lattices and fully random networks. They possess a large degree of local clustering, but a relatively small minimal path length connecting nodes throughout the system. On the other hand, scale-free networks are characterized by the presence of "hubs" or elements with an extremely high connectivity. These hubs hold the network together and produce a very small minimal path length. Complex networks are currently under intense investigation as useful structures on which to model a variety of network related phenomena, including electrical power grids, the Internet, human social relationships, proteomic, and genetic interactions, to mention just a few examples [22–26]. We are interested here in exploring the effects that arise on the static annihilation process from the different features associated with the different network topologies mentioned above.

Several exact results have previously been obtained for the static annihilation problem on ordered lattices. Kenkre and Van Horn [10] e.g., considered a one-dimensional (1D) ordered ring of N sites, in which each site is initially occupied by a particle, as in Fig. 1(a). At the onset of the annihilation process, neighboring particles on the ring begin to undergo mutual annihilation with rate constant α. As pairs of particles disappear from the ring, the possibility arises for particles at certain sites to become isolated. Such particles end up surviving indefinitely, with no neighbors left on either
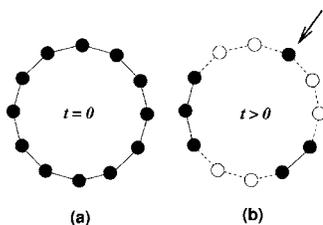
FIG. 1. Schematic diagram illustrating the annihilation process in a 1D ring. (a) At time $t=0$ there are N particles placed along the ring (black circles). (b) As time goes by, pairs of neighboring particles annihilate at a constant rate α. At some time $t>0$ some pairs have been annihilated (open circles). Note that all the neighbors of the particle signaled with an arrow have been annihilated. Since this particle has no neighbors left to annihilate with, it will survive indefinitely.

side to annihilate with [see Fig. 1(b)]. For this model the authors of Refs. [10,11] were able to calculate exactly the average fraction $f(t)$ of sites on the ring that remain populated at time t. For an infinite 1D ring they found

$$f(t) = \exp(2e^{-\alpha t} - 2), \qquad (1)$$

from which the exact stationary survival fraction

$$f_\infty = \lim_{t \to \infty} f(t) = e^{-2} \qquad (2)$$

follows. A dynamical mean-field theory for higher-dimensional ordered structures was later given by Kenkre [11]. In that work, the long-time survival fraction on a square lattice in D dimensions was found to decrease as the dimensionality D (and the number of potential annihilation partners) increases, specifically, via

$$f_\infty = (2D - 1)^{D/(1-D)}. \qquad (3)$$

Of course, on a translationally invariant structure the connectivity of any site on the lattice is the same as that of any other. Each site, moreover, has *a priori* the same probability of ultimately surviving the annihilation onslaught. It is interesting, therefore, to see what effects are generated in the annihilation dynamics by *dispersion* in the local site coordination number. In a sense, Poisson, scale-free, and small-world networks are ideal structures on which to explore these questions. Such structures allow, through a simple variation of the network parameters, significant changes in the average coordination number as well as a means to systematically change the associated dispersion in local coordination. This is especially true for scale-free networks, where the dispersion in the local coordination number can become infinite.

In the present paper we generalize the results of [10,11] to a variety of complex networks that allow us to explore these connectivity-related issues. First, in Sec. II we present a mean-field theory of the annihilation process on disordered networks with arbitrary connectivity distributions. We then apply the general formalism to three specific cases: (a) random networks in which every element has exactly K connections (Kronecker networks); (b) Erdös-Rényi (i.e., Poisson) networks with average connectivity K; and (c) scale-free networks. It is worth mentioning that the mean-field approach

requires the statistical independence of the network elements. Thus, our formalism applies neither to ordered lattices nor to small-world networks, where loops of connected sites are commonly found. Such loops generate nontrivial correlations between the elements which are not taken into account in the mean-field approach. However, case (a) above can be considered as an approximation to ordered lattices with coordination number K. The approximation becomes exact in the limit $K \to \infty$. Additionally, as we show through numerical simulation in Sec. III, the mean-field approach qualitatively describes the annihilation dynamics in ordered and small-world structures. We end this work in Sec. IV with a summary and discussion of our results.

II. MEAN-FIELD THEORY

In this section we develop a simple mean-field theory of particle annihilation in networks with an arbitrary connectivity distribution $P(k)$. This theory is exact as long as the connecting sites of each element in the network are randomly chosen from anywhere in the system. In such a case, the correlations that arise due to the occurrence of loops of connected sites can be neglected. The above is not true in general either for small-world networks or for ordered lattices. However, the mean-field approach presented here will allow us to gain insight into the effects that the overall connectivity of the system has on the annihilation dynamics. As we will see, since the infinite 1D ordered lattice with nearest-neighbor connections is loopless, our predictions recover the exact solution for this structure.

We are interested in evaluating the fraction of surviving sites $f(t)$ at time t in a network in which dimers (i.e., pairs of connected sites) have been removed randomly. We assume that the network is initially full, and that the probability that a site has k connections is given by $P(k)$.

We denote by $f(k,t)$ the fraction of surviving sites that are connected to k surviving sites at time t. We will refer to these as k sites. It is clear that $f(k,t=0)=P(k)$. Next, we determine the time evolution of these densities by considering the three different ways in which $f(k,t)$ can change:

1. As we remove dimers, a k site can become a $(k-1)$ site if one of its connecting sites is removed. To determine the rate at which this happens we focus on one of the k connections of the k site [dashed line in Fig. 2(b)]. The probability that this connection goes to a m site is proportional to $mf(m,t)$ [32]. We have to normalize this probability by dividing between $\sum_{m=1}^\infty mf(m,t)$ since the fractions $f(m,t)$ change in time and they do not add up to 1 (except at $t=0$). Therefore, the chosen connecting site in Fig. 2(b) will be a m site with probability $mf(m,t)/\sum_{m=1}^\infty mf(m,t)$. The m site will be removed if the dimer formed by this site and any of the other $(m-1)$ sites to which it is connected (not considering the k site we started from) is removed. Adding over all m and considering the k connections of the k site, the total rate at which k sites become $(k-1)$ sites is

$$kf(k,t) \frac{\displaystyle\sum_{m=0}^\infty m(m-1)f(m,t)}{\displaystyle\sum_{m=0}^\infty mf(m,t)}.$$

2. A $(k+1)$ site can become a k site. For the same reasons as before, this happens with probability

$$(k+1)f(k+1,t)\frac{\sum\limits_{m=0}^{\infty}m(m-1)f(m,t)}{\sum\limits_{m=0}^{\infty}mf(m,t)}.$$

3. Finally, k sites may also be removed if any of the k different dimers to which they belong is chosen for removal, which occurs with probability $kf(k,t)$.

Adding the three quantities above (with the correct sign) we find that the densities $f(k,t)$ satisfy the following set of evolution equations:

$$\frac{\partial f(k,t)}{\partial t} = [(k+1)f(k+1,t)-kf(k,t)]\frac{\sum\limits_{m=0}^{\infty}m(m-1)f(m,t)}{\sum\limits_{m=0}^{\infty}mf(m,t)}$$

$$-kf(k,t). \qquad (4)$$

The above equations can be treated by generating functions as follows. Let $F(z,t)$ be the generating function defined as

$$F(z,t) = \sum_{k=0}^{\infty} z^k f(k,t). \qquad (5)$$

Note that $f(t)=F(1,t)=\sum_{k=0}^{\infty}f(k,t)$ is just the overall fraction of surviving elements at time t. From Eq. (4) it follows that $F(z,t)$ satisfies the equation

$$\frac{\partial F(z,t)}{\partial t} = [(1-z)g(t)-z]\frac{\partial F(z,t)}{\partial z}, \qquad (6)$$

where

$$g(t)=\frac{\sum\limits_{m=0}^{\infty}m(m-1)f(m,t)}{\sum\limits_{m=0}^{\infty}mf(m,t)}=\left[\frac{\left(\dfrac{\partial^2 F(z,t)}{\partial z^2}\right)}{\left(\dfrac{\partial F(z,t)}{\partial z}\right)}\right]_{z=1}. \qquad (7)$$

Equation (6) can be solved by the method of characteristics, which gives

$$F(z,t)=Q\left(1+(z-1)e^{-G(t)}-\int_0^t e^{-G(\tau)}d\tau\right), \qquad (8)$$

where

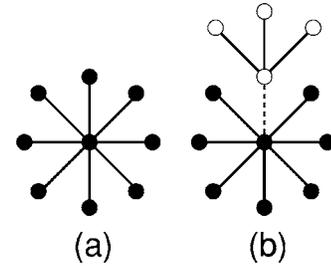$$G(t)=t+\int_0^t g(\tau)d\tau, \qquad (9)$$

and

FIG. 2. (a) A k site (at the center) with k connecting sites. $k=8$ in this diagram. (b) One of the connecting sites of the k site is a m site with m connections ($m=4$ in the diagram). The probability that an arbitrary connection (dashed line) of the k site goes to a m site is $mf(m,t)/\Sigma_{m=0}^{\infty}mf(m,t)$.

$$Q(z) = \sum_{k=0}^{\infty} z^k P(k). \qquad (10)$$

Note that $Q(z)$ is the generating function of the initial distribution $P(k)$. It is also important to note that $g(t)$ must be determined through the consistency Eq. (7).

It is clear that at the end of the annihilation process, only isolated elements with $k=0$ will survive. Therefore, the fractions $f(k,t)$ should fulfill the condition

$$\lim_{t\to\infty}f(k,t) = 0 \quad \text{for all} \quad k \geq 1.$$

The fraction f_∞ of surviving elements at the end of the annihilation process is then given by

$$f_\infty = \lim_{t\to\infty}f(0,t) = \lim_{t\to\infty}F(1,t). \qquad (11)$$

In what follows we apply the general formalism presented in this section to obtain f_∞ for networks with different topologies.

A. Kronecker delta distribution

We now apply the preceding formalism to the specific case in which every site of the initial network has exactly K connections. Therefore, the initial distribution $P(k)$ is given by a Kronecker delta function: $P(k)=\delta_{k,K}$. This case can be considered as an approximation to an ordered lattice with coordination number K. Such an approximation becomes exact for $K\to\infty$. However this case is particularly interesting when $K=2$ because, given that in the "thermodynamic" limit there are no loops of connected sites in the network, the system corresponds exactly to the infinite 1D lattice with nearest-neighbor connections, for which the exact solution is known [see Eqs. (1) and (2) and Refs. [10,11]]. For this choice of the initial distribution, Eq. (10) becomes

$$Q(z) = \sum_{k=0}^{\infty} z^k P(k) = z^K.$$

From this result we find that the generating function for the distribution of k sites, Eq. (8), is given by

$$F(z,t) = \left[1 + (z-1)e^{-G(t)} - \int_0^t e^{-G(\tau)}d\tau \right]^K, \quad (12)$$

and the consistency Eq. (7) becomes

$$g(t) = -(K-1)\frac{d}{dt}\ln\left(1 - \int_0^t e^{-G(\tau)}d\tau\right). \quad (13)$$

To solve the preceding integral equation we first integrate it from 0 to t, which gives

$$\int_0^t g(\tau)d\tau = -(K-1)\ln\left[1 - \int_0^t e^{-G(\tau)}d\tau\right],$$

or, equivalently,

$$\exp\left[-\int_0^t g(\tau)d\tau\right] = \left(1 - \int_0^t e^{-G(\tau)}d\tau\right)^{K-1}.$$

Multiplying both sides of the above equation by e^{-t} we obtain

$$e^{-G(t)} = e^{-t}\left(1 - \int_0^t e^{-G(\tau)}d\tau\right)^{K-1}, \quad (14)$$

where we have used the definition of $G(t)$ given in Eq. (9). The following change of variable will be very useful to solve the integral equations:

$$u(t) = 1 - \int_0^t e^{-G(\tau)}d\tau. \quad (15)$$

With this change of variable, Eq. (14) can be written as

$$\frac{du(t)}{dt} = -e^{-t}[u(t)]^{K-1}. \quad (16)$$

The above equation can be solved easily. However, care must be taken for the case $K=2$, which must be evaluated separately. Assuming $K>2$ first, the solution of Eq. (16) with the initial condition $u(0)=1$ is

$$u(t) = [1 + (K-2)(1-e^{-t})]^{1/(2-K)}. \quad (17)$$

Although the complete hierarchy of distributions $f(k,t)$ can be obtained from the preceding results, at this point we are interested in the final fraction of surviving sites f_∞. This can be readily computed by noting from Eqs. (12) and (15) that the overall fraction $f(t)=F(1,t)$ of surviving sites at time t is

$$f(t) = [u(t)]^K = [1 + (K-2)(1-e^{-t})]^{K/(2-K)}.$$

Taking the limit $t\rightarrow\infty$ in the above equation we obtain

$$f_\infty = (K-1)^{K/(2-K)} \quad (K>2). \quad (18)$$

Since a square lattice in D dimensions has coordination number $K=2D$, the above result coincides with Eq. (3), which was reported in Ref. [11].

As mentioned before, the case $K=2$ has to be evaluated separately. For $K=2$, the solution of Eq. (16) with the initial condition $u(0)=1$ is
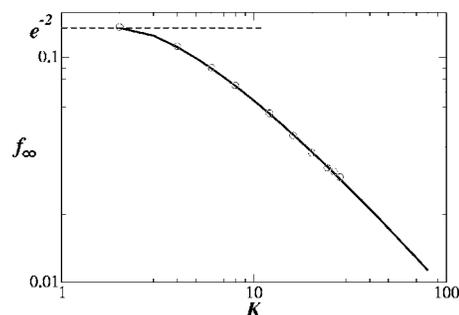

FIG. 3. Fraction of surviving elements f_∞ as a function of the average network connectivity K for networks with Kronecker distribution. The circles are the plot of the simulation data whereas the solid curve is the graph of the theoretical prediction given in Eqs. (18) and (20). The dashed line indicates the value e^{-2} corresponding to the 1D ring with nearest-neighbor interactions. To generate the simulation data we used networks with $N=10^3$ sites. Each point is the average over 100 realizations.

$$u(t) = \exp(e^{-t} - 1). \quad (19)$$

Therefore, the overall fraction $f(t)$ of surviving sites in this case becomes

$$f(t) = [u(t)]^2 = \exp(2e^{-t} - 2),$$

which, in the limit $t\rightarrow\infty$, gives

$$f_\infty = e^{-2} \quad (K=2). \quad (20)$$

This is the exact result for the 1D lattice with nearest-neighbor connections. [See Eq. (2) and Refs. [10,11].]

Figure 3 shows f_∞ as a function of K. The solid curve is the theoretical result as predicted in Eqs. (18) and (20), whereas the circles correspond to the computer simulation data. Note from Eq. (18) that $f_\infty \sim 1/K$ for large values of K, and therefore

$$\lim_{K\rightarrow\infty} f_\infty = 0.$$

So, the more connected the initial network, the smaller the fraction of surviving sites at the end of the annihilation process.

For the sake of completeness, we compute the explicit form of the distributions $f(k,t)$ for the case $K>2$. To this end, we rewrite Eqs. (15) and (16) as

$$e^{-G(t)} = e^{-t}[u(t)]^{K-1},$$

$$\int_0^t e^{-G(\tau)}d\tau = 1 - u(t).$$

Substituting the above expressions into Eq. (12) we obtain for the generating function

$$F(z,t) = [(z-1)e^{-t}[u(t)]^{K-1} + u(t)]^K,$$

which, after expanding in powers of z using the binomial theorem, transforms into

$$F(z,t) = \sum_{k=0}^{K} \binom{K}{k} \frac{(u(t) - e^{-t}[u(t)]^{K-1})^K}{(e^t[u(t)]^{2-K} - 1)^k} z^k.$$
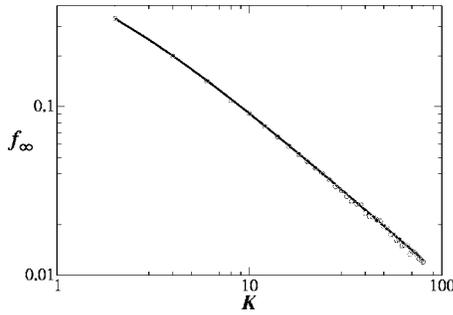
FIG. 4. Fraction of surviving elements f_∞ as a function of the average network connectivity K for Erdös-Rényi networks with Poisson distribution. The circles are the plot of the simulation data whereas the solid curve is the graph of the theoretical prediction given in Eq. (29). Each point of the simulation data is the average over 100 realizations using networks with $N=10^3$ sites.

From this result it follows immediately that the distribution $f(k,t)$ of surviving sites with k connections at time t is given by

$$f(k,t) = \binom{K}{k} \frac{(u(t) - e^{-t}[u(t)]^{K-1})^K}{(e^t[u(t)]^{2-K} - 1)^k}, \quad (21)$$

where for $u(t)$ we have to use Eq. (17) if $K>2$, or Eq. (19) if $K=2$. In any case, from Eq. (21) we can see that $\lim_{t\to\infty} f(k,t)=0$ for all $k \geq 1$. Namely, at the end of the annihilation process, only isolated sites with $k=0$ survive, as expected. However, for $k \geq 1$ the rate at which $f(k,t) \to 0$ as $t \to \infty$ depends on the value of k. To see this, consider the distributions $f(k,t)$ and $f(k',t)$ with $k>k'$. Then, from Eq. (21) we get

$$\lim_{t\to\infty} \frac{f(k,t)}{f(k',t)} \sim \lim_{t\to\infty} \frac{1}{(e^t[u(t)]^{2-K} - 1)^{k-k'}} = 0.$$

This result shows that more connected sites annihilate faster than less connected ones, as expected.

B. Poisson distribution

Next we treat the case in which the initial distribution of connections is Poisson with mean K: $P(k)=e^{-K}K^k/k!$. This case corresponds to the Erdös-Rényi topology, for which $Q(z)$ becomes

$$Q(z) = \sum_{k=0}^{\infty} z^k P(k) = e^{-K}\sum_{k=0}^{\infty} z^k \frac{K^k}{k!} = e^{-K(1-z)}. \quad (22)$$

Using this result in Eq. (8) we obtain

$$F(z,t) = \exp\left[-K\left((1-z)e^{-G(t)} + \int_0^t e^{-G(\tau)}d\tau\right)\right], \quad (23)$$

and the consistency Eq. (7) in this case is

$$g(t) = K\exp\left\{-t - \int_0^t g(\tau)d\tau\right\} = Ke^{-G(t)}. \quad (24)$$

The above integral equation can be easily solved for $g(t)$, obtaining

$$g(t) = \frac{Ke^{-t}}{1 + K(1 - e^{-t})}. \quad (25)$$

From Eq. (24) we have $e^{-G(t)}=g(t)/K$, from which it follows that

$$e^{-G(t)} = \frac{e^{-t}}{1 + K(1 - e^{-t})},$$

$$\int_0^t e^{-G(\tau)}d\tau = \frac{1}{K}\ln\{1 + K(1 - e^{-t})\}.$$

Substituting the above results into Eq. (23) we obtain

$$F(z,t) = \frac{e^{-g(t)}}{1 + K(1 - e^{-t})}e^{g(t)z} \quad (26)$$

$$= \frac{e^{-g(t)}}{1 + K(1 - e^{-t})}\sum_{k=0}^{\infty} \frac{[g(t)]^k}{k!}z^k, \quad (27)$$

where we have used the fact that $g(t)=Ke^{-G(t)}$. It follows immediately from Eq. (27) that the distribution $f(k,t)$ of k sites at time t is

$$f(k,t) = \frac{e^{-g(t)}}{1 + K(1 - e^{-t})}\frac{[g(t)]^k}{k!}. \quad (28)$$

An interesting aspect of this result is the fact that the distribution of k sites continues to be Poissonian (though not normalized) throughout the evolution of the system. Note also that, since $\lim_{t\to\infty} g(t)=0$ [see Eq. (25)], it follows from Eq. (28) that $\lim_{t\to\infty} f(k,t)=0$ for all $k \geq 1$, as expected. Again, the rate at which this happens depends on the value of the connectivity k. Indeed, considering the distributions $f(k,t)$ and $f(k',t)$, with $k>k'$, from Eq. (28) and the fact that $g(t) \to 0$ as $t \to \infty$, we obtain

$$\lim_{t\to\infty} \frac{f(k,t)}{f(k',t)} \sim \lim_{t\to\infty} [g(t)]^{k-k'} = 0.$$

Therefore, the higher the connectivity of a given site, the faster it annihilates.

The overall fraction $f(t)$ of surviving sites at time t, regardless of their connectivity, is obtained from Eq. (26) with $z=1$, which gives

$$f(t) = F(1,t) = \frac{1}{1 + K(1 - e^{-t})}.$$

Finally, the fraction f_∞ of surviving sites at the end of the annihilation process can be obtained from the above equation [or from Eq. (28) with $k=0$] by taking the limit $t \to \infty$. We obtain

$$f_\infty = \frac{1}{1 + K}. \quad (29)$$

Figure 4 shows the graph of f_∞ as a function of K. The solid curve is the plot of the theoretical prediction given in Eq. (29) and the circles correspond to the simulation data. Note that, once again

$$\lim_{K \to \infty} f_\infty = 0,$$

as for the Kronecker-delta case.

C. Scale-free distribution

In this section we consider scale-free networks for which the initial distribution of connections acquires the form

$$P(k) = \frac{1}{\zeta(\gamma)} k^{-\gamma},$$

where $\zeta(\gamma) = \sum_{k=1}^{\infty} k^{-\gamma}$ is the Riemann zeta function. In this case, the generating function (10) of the initial distribution becomes

$$Q(z) = \sum_{k=1}^{\infty} z^k P(k) = \frac{1}{\zeta(\gamma)} \sum_{k=1}^{\infty} \frac{z^k}{k^\gamma} = \frac{1}{\zeta(\gamma)} \mathrm{Li}_\gamma(z), \quad (30)$$

where $\mathrm{Li}_\gamma(z) = \sum_{k=1}^{\infty} z^k / k^\gamma$ is the polylogarithm function of order γ. This function has the following properties, which will be of use for further analysis:

$$\mathrm{Li}_\gamma(0) = 0; \quad (31a)$$

$$\mathrm{Li}_\gamma(1) = \zeta(\gamma); \quad (31b)$$

$$\frac{\partial \mathrm{Li}_\gamma(z)}{\partial z} = \frac{1}{z} \mathrm{Li}_{\gamma-1}(z); \quad (31c)$$

$$\frac{\partial^2 \mathrm{Li}_\gamma(z)}{\partial z^2} = \frac{1}{z^2} [\mathrm{Li}_{\gamma-2}(z) - \mathrm{Li}_{\gamma-1}(z)]. \quad (31d)$$

The generating function $F(z,t)$ for this case is

$$F(z,t) = \frac{1}{\zeta(\gamma)} \mathrm{Li}_\gamma \left(1 + (z-1)e^{-G(t)} - \int_0^t e^{-G(\tau)} d\tau \right), \quad (32)$$

and, using properties (31c) and (31d), the consistency Eq. (7) becomes

$$g(t) = \frac{e^{-G(t)}}{u(t)} \frac{\mathrm{Li}_{\gamma-2}[u(t)] - \mathrm{Li}_{\gamma-1}[u(t)]}{\mathrm{Li}_{\gamma-1}[u(t)]}, \quad (33)$$

where $u(t)$ is defined as in Eq. (15). Note from Eqs. (32) and (15) that the overall fraction $f(t)$ of surviving particles at time t is given by

$$f(t) = F(1,t) = \frac{1}{\zeta(\gamma)} \mathrm{Li}_\gamma[u(t)]. \quad (34)$$

Therefore, to compute $f(t)$ we first have to know $u(t)$. In order to do so, we rewrite the consistency Eq. (33) as

$$g(t) = \frac{d}{dt} \{ \ln[u(t)] - \ln(\mathrm{Li}_{\gamma-1}[u(t)]) \},$$

where we have used the fact that $du(t)/dt = -e^{-G(t)}$. The last equation can be integrated from 0 to t taking into account that $u(0) = 1$, which leads to

$$\int_0^t g(t) dt = \ln \left(\frac{u(t)}{\mathrm{Li}_{\gamma-1}[u(t)]} \right) + \ln[\zeta(\gamma-1)].$$

Adding t on both sides of the previous equation and exponentiating we get

$$e^{-G(t)} = \frac{\mathrm{Li}_{\gamma-1}[u(t)]}{u(t)} \frac{e^{-t}}{\zeta(\gamma-1)},$$

or equivalently,

$$\frac{u(t)}{\mathrm{Li}_{\gamma-1}[u(t)]} \frac{du(t)}{dt} = -\frac{e^{-t}}{\zeta(\gamma-1)}. \quad (35)$$

We have been so far unable to find an exact analytical solution to the above nonlinear differential equation. However, we can solve it numerically to obtain the asymptotic value $u_\infty = \lim_{t \to \infty} u(t)$ with any desired accuracy. Once u_∞ has been determined, it follows from Eq. (34) that the final fraction f_∞ of surviving particles at the end of the annihilation process will be given by

$$f_\infty = \frac{1}{\zeta(\gamma)} \mathrm{Li}_\gamma(u_\infty). \quad (36)$$

In order to determine u_∞, we first integrate Eq. (35) from 0 to t, which gives

$$\int_{u(t)}^1 \frac{u'}{\mathrm{Li}_{\gamma-1}(u')} du' = \frac{1}{\zeta(\gamma-1)} (1 - e^{-t}).$$

Taking the limit $t \to \infty$ in the previous equation we obtain

$$\int_{u_\infty}^1 \frac{u'}{\mathrm{Li}_{\gamma-1}(u')} du' = \frac{1}{\zeta(\gamma-1)}. \quad (37)$$

An important conclusion can immediately be drawn from this equation. Note that, since $\zeta(\gamma-1) = \infty$ for $1 < \gamma \le 2$, the above equation in this range becomes

$$\int_{u_\infty}^1 \frac{u'}{\mathrm{Li}_{\gamma-1}(u')} du' = 0 \quad \text{for} \quad 1 < \gamma \le 2,$$

which has the solution $u_\infty = 1$. From Eq. (36) and property (31b), we obtain

$$f_\infty = 1 \quad \text{for} \quad 1 < \gamma \le 2.$$

In other words, *essentially all the particles of a scale-free network with infinite average connectivity survive the annihilation process*. This result is easy to interpret. What holds a scale-free network together are the "hubs," i.e., the sites with an extremely high number of connections [14]. But the hubs represent a negligible fraction of the total number of sites in the network. However, a randomly chosen site will be connected to a hub with certainty. Therefore, in this range of values of γ, the hubs are annihilated from the very beginning of the process. But once the hubs have been annihilated, the network disintegrates and only isolated sites are left. Hence, $f_\infty = 1$ in the thermodynamic limit.

To obtain f_∞ for $\gamma > 2$ it is convenient to define the function $I_\gamma(u)$ as
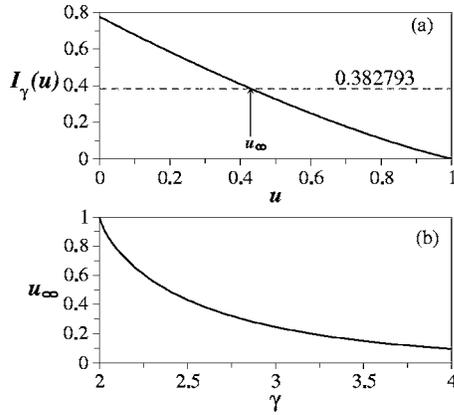
FIG. 5. Features in scale-free networks. (a) The solid curve is the graph of $I_\gamma(u)$ [defined in Eq. (38)] as a function of u for the case $\gamma=2.5$. The dashed line indicates the value $1/\zeta(1.5)$ $\approx 0.382\,793$, whose intersection with $I_\gamma(u)$ in this case gives u_∞ ≈ 0.431. (b) u_∞ as a function of γ. This curve was obtained by solving numerically the transcendental Eq. (39).

$$I_\gamma(u) = \int_u^1 \frac{u'}{\mathrm{Li}_{\gamma-1}(u')} du'. \tag{38}$$

With this definition, Eq. (37) can be written as

$$I_\gamma(u_\infty) = \frac{1}{\zeta(\gamma-1)}. \tag{39}$$

This is a transcendental equation for u_∞. Note that $I_\gamma(u)$ is a continuous monotonically decreasing function of u. For example, the solid line in Fig. 5(a) is the graph of $I_\gamma(u)$ for $\gamma=2.5$, whereas the dashed line indicates the value of $1/\zeta(\gamma-1)$, which for $\gamma=2.5$ is $1/\zeta(1.5) \approx 0.382\,793$. Then, u_∞ is the value of u at which the solid curve intersects the dashed one, which for the case shown in Fig. 5(a), is $u_\infty \approx 0.431$. Since $I_\gamma(u)$ is a "well behaved" function for every γ, we can find the roots of Eq. (39) with any desired accuracy. Figure 5(b) shows u_∞ as a function of γ. Using these results in Eq. (36), we obtain the data reported in Fig. 6(a), in which f_∞ is plotted as a function of γ. The solid curve depicts the theoretical result and the circles are data from the simulation of the system in the computer. The small difference between the theoretical prediction and the simulation at $\gamma=2$ is due to finite size effects in the computer simulation.

Finally, Fig. 6(b) shows the graph of f_∞ as a function of the average network connectivity K, which for scale-free networks is given by $K=\zeta(\gamma-1)/\zeta(\gamma)$. Note that f_∞ *increases* with K and asymptotically approaches its maximum value $f_\infty=1$ as $K\to\infty$. As explained before, due to the presence of "hubs" in scale-free networks, we have

$$\lim_{K\to\infty} f_\infty = 1,$$

contrary to what happens in Kronecker and Poisson networks, for which $\lim_{K\to\infty} f_\infty = 0$.

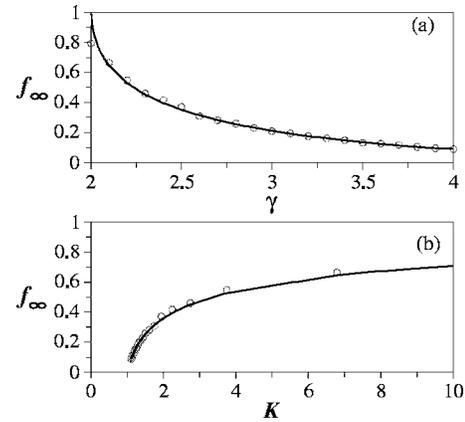FIG. 6. (a) Surviving fraction f_∞ in scale-free networks as a function of γ. The solid curve corresponds to the theoretical result as predicted by Eqs. (36) and (37), whereas the circles are the data obtained from computer simulation. The simulation was carried out for networks with $N=10^4$ sites. Each point is the average over 100 realizations. (b) Same data as before but plotted against the average network connectivity $K=\zeta(\gamma-1)/\zeta(\gamma)$.

III. EXTENSION TO SMALL-WORLD NETWORKS

Small-world networks pose a special challenge for analylicalal treatment since we have to deal with both ordered short-range and random long-range interactions simultaneously. Although some analytical results have been obtained for percolation and ferromagneticlike systems in small-world networks [27–30], to the best of our knowledge there does not yet exist a general formalism to study the dynamical properties of this kind of networks given a specific interaction rule between the elements. In particular, for the annihilation problem we are considering, the ordered short-range connections produce "loops" of connected sites, which in turn give rise to nontrivial correlations between the elements. Such correlations are not taken into account in the mean-field theory we have presented. Therefore, we do not expect our formalism to be exactly applicable to small-world networks.

However, since small-world networks can be considered as something between ordered lattices and fully random networks, we do expect the static annihilation process in SW structures to be similar to that in Kronecker or Poisson networks. In this section we present results obtained from the numerical simulation of the system on small-world networks. Such networks are constructed by starting with an ordered ring of N sites and connectivity K in which each site is connected to its $K/2$ nearest neighbors on the left and $K/2$ nearest neighbors on the right. Disorder is then introduced into this ordered structure by disconnecting with probability p each bond in the lattice emerging from a given site and reconnecting it to another randomly chosen site to which it was not originally connected (provided that the rewiring does not result in two or more disconnected subnetworks).

Thus, the reconnection or rewiring probability p is a measure of the disorder of the system, and allows the system to be tuned from a completely ordered ($p=0$) to a completely disordered ($p=1$) structure. It is also a direct measure of the number of "shortcuts" that exist in the network. Note that the
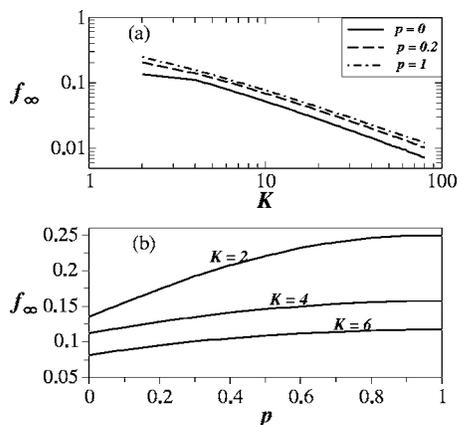
FIG. 7. (a) Surviving fraction f_∞ in small-world networks as a function of K for three values of the rewiring probability. These three values correspond to an ordered ring ($p=0$), a small-world network with 20% of shortcuts ($p=0.2$), and a fully random network ($p=1$). (b) Fraction of surviving elements f_∞ as a function of p for three values of the average network connectivity K. In both figures the data were computed numerically through computer simulation using networks with $N=10^3$ sites. Each point is the average over 1000 realizations.

rewiring algorithm leaves the average connectivity K associated with the original ordered structure unchanged, but changes the dispersion in the local connectivity. Indeed, after rewiring, any given site may be connected to a greater or fewer number of sites than before rewiring. Therefore, the average connectivity and the magnitude of fluctuations in the local connectivity are independently adjustable through the parameters K and p.

Figure 7(a) shows f_∞ as a function of K for three different values of the rewiring probability: $p=0$ (ordered ring), $p=0.2$ (small-world network), and $p=1$ (fully random network). Note that f_∞ behaves as $f_\infty \sim 1/K$ for large values of K regardless of the value of the rewiring probability p. Therefore, small-world networks behave like Kronecker and Poisson networks. On the other hand, Fig. 7(b) shows f_∞ as a function of p for three values of the average network connectivity K. Interestingly, the numerical results of this figure indicate that the fraction f_∞ of surviving particles *increases* with an increasing number of small-world shortcuts. One might think that such shortcuts would enhance particle annihilation between sites very far away, and thereby lead to a decrease in the survival fraction. However, in order for a small-world network to achieve the short path length with which it is associated, a significant number of sites have to be more connected than others in the system. Such sites act as gateways, allowing access across the system from any direction. Since the average network connectivity is preserved during rewiring, the existence of highly connected elements implies the existence of many elements with a connectivity smaller than average. Consequently, there will exist situations in which sites with high connectivity are connected to many sites of below average connectivity. As our mean-field formalism shows, a highly connected site is very likely to annihilate quickly with one of its many partners, leaving the remaining sites to which it was connected more

isolated than they would have been if they had been part of an ordered network. Hence, it appears that dispersion in the local connectivity leads to enhanced survivability in the annihilation problem.

IV. SUMMARY AND DISCUSSION

In this work he have analyzed the static annihilation process on complex networks. In this problem, pairs of connected particles annihilate at a constant rate. Through a mean-field approach we were able to compute exact general expressions for the fraction of surviving particles with k connections at time t for random networks with arbitrary connectivity distribution $P(k)$. Our results indicate that Kronecker and Poisson networks exhibit a similar behavior in that the final fraction of surviving particles f_∞ asymptotically behaves as $1/K$ for large values of K, the average connectivity of the initial network. Numerical simulations show that this is also true for ordered lattices and small-world networks. So, although the mean-field approach is not exactly applicable to ordered latices and small-world networks, it predicts qualitatively the correct asymptotic limit $f_\infty \sim 1/K$ for such systems.

The situation is radically different in scale-free networks, characterized by the connectivity distribution $P(k) \sim k^{-\gamma}$. For this kind of network, our theory predicts that $f_\infty=1$ for $1 < \gamma \le 2$ and that $\lim_{\gamma \to \infty} f_\infty=0$. Thus, in the range $1 < \gamma \le 2$ in which the average network connectivity K diverges, all the particles (or almost all in finite systems) survive the annihilation process. The above result is a consequence of the fact that highly connected sites annihilate faster than poorly connected ones. While this happens in every network, it has dramatic consequences in scale-free structures in which, once the hubs are annihilated, the network breaks apart and only isolated sites are left. This kind of behavior is reminiscent of the breakdown of scale-free networks when the highly connected sites are deliberately attacked [14]. Here we have shown that the annihilation of the hubs does not only break the network apart, but that it pulverizes the network.

Diffusion annihilation dynamics of the kind $A+A \to \varnothing$ has recently been studied on complex networks using an analogous formalism as the one presented in this work [31]. In diffusion annihilation, the particles, rather than being fixed to the vertices, are free to move (diffuse) throughout the network. Two particles annihilate if they collide at some vertex of the network for the first time. The authors of Ref. [31] show that the fraction of surviving particles decreases in time as t^{-1} for Poisson-like networks and as $t^{-\beta}$ for scale-free networks, where β depends on the scale-free exponent. Obviously, contrary to what happens in the static case considered in this work, there are no surviving particles in diffusion annihilation. Thus, our results describe situations that are, in some sense, complementary to those analyzed by Ref. [31].

[1] L. Frachebourg, P. L. Krapivsky, and S. Redner, J. Phys. A **31**, 2791 (1998).

[2] E. BenNaim, S. Redner, and P. L. Krapivsky, J. Phys. A **29**, L561 (1996).

[3] P. Avakian and R. Merrifield, Mol. Cryst. **5**, 37 (1968); N. E. Geacintov and C. E. Swenberg, in *Organic Molecular Photophysics*, edited by J. B. Birks (Willey, New Tork, 1973), Vol. I; V. M. Kenkre, in *Exciton Dynamics in Molecular Crystals and Aggregates: The Master Equation Approach*, edited by G. Hoehler Springer Tracts in Modern Physics, Vol. 94 (Springer, Berlin, 1982).

[4] T. Vicsek, A. Czirók, E. Ben-Jacob, I. Cohen, and O. Shochet, Phys. Rev. Lett. **75**, 1226 (1995).

[5] M. Aldana and C. Huepe, J. Stat. Phys. **112**, 135 (2003).

[6] J. R. Wilson and G. J. Mathews, Astrophys. J. **610**, 368 (2004).

[7] D. G. Yakovlev and K. P. Levenfish, Contrib. Plasma Phys. **43** 390 (2003).

[8] H. Kitamura, Astrophys. J. **539**, 888 (2000).

[9] J. W. Evans, Rev. Mod. Phys. **65**, 1281 (1993).

[10] V. M. Kenkre and H. M. Van Horn, Phys. Rev. A **23**, 3200 (1981).

[11] V. M. Kenkre, J. Stat. Phys. **30**, 293 (1983).

[12] J. D. Noh and H. Rieger, Phys. Rev. Lett. **92**, 118701 (2004).

[13] C. P Herrero. Phys. Rev. E **65**, 066110 (2002).

[14] R. Albert, H. Jeong, and A.-L. Barabási, Nature (London) **406**, 378 (2000).

[15] F. Jasch and A. Blumen, Phys. Rev. E **63**, 041108 (2001).

[16] M. Aldana and H. Larralde. Phys. Rev. E **70** 066130 (2004).

[17] M. F. Laguna, G. Abramson, and D. H. Zanette, Physica A **329**, 459 (2003); Complexity **9** (4), 31, (2004).

[18] M. Kuperman and G. Abramson, Phys. Rev. Lett. **86**, 2909 (2001).

[19] R. Pastor-Satorras and A. Vespignani, Phys. Rev. Lett. **86**, 3200 (2001).

[20] L. K. Gallos, Phys. Rev. E **70**, 046116 (2004).

[21] F. Jasch and A. Blumen, Phys. Rev. E **64**, 066104 (2001).

[22] D. J. Watts and S. H. Strogatz, Nature (London) **393**, 440 (1998).

[23] S. H. Strogatz, Nature (London) **410**, 268 (2001).

[24] R. Albert and A.-L. Barabási, Rev. Mod. Phys. **74**, 47 (2002).

[25] M. E. J. Newman, SIAM Rev. **45**, 167 (2003).

[26] S. N. Dorogovtsev and J. F. F. Mendes, Adv. Phys. **51**, 1079 (2002).

[27] C. Moore and M. E. J Newman, Phys. Rev. E **62**, 7059 (2000).

[28] J. Viana-Lopes, Yu. G. Pogorelov, J. M. B. Lopes dos Santos, and R. Toral, cond-mat/0402138 (unpublished).

[29] R. Nikoletopoulos, A. C. C. Cohen, I. Pérez Castillo, N. S. Skantzos, J. P. L. Hatchett, and B. Wemmenhove, J. Phys. A **37**, 6455 (2004).

[30] A. Barrat and M. Weigt, Eur. Phys. J. B **13**, 547 (2000).

[31] M. Catanzaro, M. Boguna, and R. Pastor-Satorras, cond-mat/0407447 (unpublished).

[32] The factor *m* stands for the fact that it is more probable to be connected to sites with a large number of connections than to sites with a small number of connections.